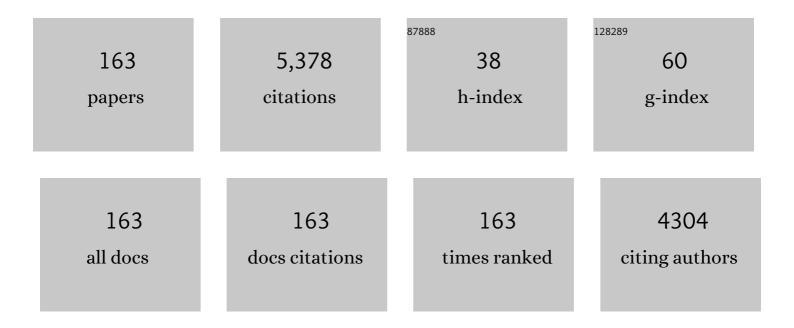
Grzegorz Lisak

List of Publications by Year in descending order

Source: https://exaly.com/author-pdf/7976642/publications.pdf Version: 2024-02-01



#	Article	IF	CITATIONS
1	Fate and distribution of heavy metals during thermal processing of sewage sludge. Fuel, 2018, 226, 721-744.	6.4	203
2	Application of conducting polymers to wound care and skin tissue engineering: A review. Biosensors and Bioelectronics, 2019, 135, 50-63.	10.1	179
3	Insights into the thermolytic transformation of lignocellulosic biomass waste to redox-active carbocatalyst: Durability of surface active sites. Applied Catalysis B: Environmental, 2018, 233, 120-129.	20.2	169
4	Heavy Metals Detection with Paper-Based Electrochemical Sensors. Analytical Chemistry, 2021, 93, 1880-1888.	6.5	127
5	Environmental perspectives of recycling various combustion ashes in cement production – A review. Waste Management, 2018, 78, 401-416.	7.4	126
6	Metal-organic frameworks for pesticidal persistent organic pollutants detection and adsorption – A mini review. Journal of Hazardous Materials, 2021, 413, 125325.	12.4	119
7	Characteristics of incineration ash for sustainable treatment and reutilization. Environmental Science and Pollution Research, 2019, 26, 16974-16997.	5.3	113
8	Chemical recycling of plastic waste for sustainable material management: A prospective review on catalysts and processes. Renewable and Sustainable Energy Reviews, 2022, 154, 111866.	16.4	110
9	Processing of flexible plastic packaging waste into pyrolysis oil and multi-walled carbon nanotubes for electrocatalytic oxygen reduction. Journal of Hazardous Materials, 2020, 387, 121256.	12.4	103
10	Activated multi-walled carbon nanotubes decorated with zero valent nickel nanoparticles for arsenic, cadmium and lead adsorption from wastewater in a batch and continuous flow modes. Journal of Hazardous Materials, 2022, 423, 126993.	12.4	96
11	Effects of sewage sludge organic and inorganic constituents on the properties of pyrolysis products. Energy Conversion and Management, 2019, 196, 1410-1419.	9.2	89
12	Insights into the speciation of heavy metals during pyrolysis of industrial sludge. Science of the Total Environment, 2019, 691, 232-242.	8.0	86
13	Environmental impact assessment of converting flexible packaging plastic waste to pyrolysis oil and multi-walled carbon nanotubes. Journal of Hazardous Materials, 2020, 390, 121449.	12.4	86
14	Taguchi optimization design of diameter-controlled synthesis of multi walled carbon nanotubes for the adsorption of Pb(II) and Ni(II) from chemical industry wastewater. Chemosphere, 2021, 266, 128937.	8.2	83
15	A hot syngas purification system integrated with downdraft gasification of municipal solid waste. Applied Energy, 2019, 237, 227-240.	10.1	76
16	Lead(II)-selective ionophores for ion-selective electrodes: A review. Analytica Chimica Acta, 2013, 791, 1-12.	5.4	70
17	Inorganic salt modified paper substrates utilized in paper based microfluidic sampling for potentiometric determination of heavy metals. Sensors and Actuators B: Chemical, 2019, 290, 347-356.	7.8	64
18	Life cycle assessment of plastic grocery bags and their alternatives in cities with confined waste management structure: A Singapore case study. Journal of Cleaner Production, 2021, 278, 123956.	9.3	63

#	Article	IF	CITATIONS
19	Upgrading of non-condensable pyrolysis gas from mixed plastics through catalytic decomposition and dechlorination. Fuel Processing Technology, 2018, 170, 13-20.	7.2	59
20	Plastic derived carbon nanotubes for electrocatalytic oxygen reduction reaction: Effects of plastic feedstock and synthesis temperature. Electrochemistry Communications, 2019, 101, 11-18.	4.7	59
21	Effect of biochars on bioaccumulation and human health risks of potentially toxic elements in wheat (Triticum aestivum L.) cultivated on industrially contaminated soil. Environmental Pollution, 2020, 260, 113887.	7.5	59
22	In situ grown metallic nickel from X–Ni (X=La, Mg, Sr) oxides for converting plastics into carbon nanotubes: Influence of metal–support interaction. Journal of Cleaner Production, 2020, 258, 120633.	9.3	58
23	PVC-Based Ion-Selective Electrodes with a Silicone Rubber Outer Coating with Improved Analytical Performance. Analytical Chemistry, 2019, 91, 10524-10531.	6.5	57
24	Highly reproducible solid contact ion selective electrodes: Emerging opportunities for potentiometry – A review. Analytica Chimica Acta, 2021, 1162, 338304.	5.4	57
25	Paper-based microfluidic sampling for potentiometric determination of ions. Sensors and Actuators B: Chemical, 2015, 207, 933-939.	7.8	56
26	Enhanced activation of peroxydisulfate by CuO decorated on hexagonal boron nitride for bisphenol A removal. Chemical Engineering Journal, 2020, 393, 124714.	12.7	55
27	Poisoning effects of H2S and HCl on the naphthalene steam reforming and water-gas shift activities of Ni and Fe catalysts. Fuel, 2019, 241, 1008-1018.	6.4	54
28	Advanced sensing technologies of phenolic compounds for pharmaceutical and biomedical analysis. Journal of Pharmaceutical and Biomedical Analysis, 2020, 179, 112913.	2.8	53
29	Carbon based copper(II) phthalocyanine catalysts for electrochemical CO2 reduction: Effect of carbon support on electrocatalytic activity. Carbon, 2020, 168, 245-253.	10.3	53
30	Multi-heteroatom-doped carbocatalyst as peroxymonosulfate and peroxydisulfate activator for water purification: A critical review. Journal of Hazardous Materials, 2022, 426, 128077.	12.4	53
31	Potentiometric sensing utilizing paper-based microfluidic sampling. Analyst, The, 2014, 139, 2133-2136.	3.5	51
32	Thermodynamic analyses of synthetic natural gas production via municipal solid waste gasification, high-temperature water electrolysis and methanation. Energy Conversion and Management, 2019, 202, 112160.	9.2	46
33	Accelerated organics degradation by peroxymonosulfate activated with biochar co-doped with nitrogen and sulfur. Chemosphere, 2021, 277, 130313.	8.2	43
34	Sponge-based microfluidic sampling for potentiometric ion sensing. Analytica Chimica Acta, 2019, 1091, 103-111.	5.4	42
35	Bamboo-like N-doped carbon nanotube–confined cobalt as an efficient and robust catalyst for activating monopersulfate to degrade bisphenol A. Chemosphere, 2021, 279, 130569.	8.2	42
36	The use of fly ashes from waste-to-energy processes as mineral CO2 sequesters and supplementary cementitious materials. Journal of Hazardous Materials, 2020, 398, 122906.	12.4	42

#	Article	IF	CITATIONS
37	Solid-contact lead(II) ion-selective electrodes for potentiometric determination of lead(II) in presence of high concentrations of Na(I), Cu(II), Cd(II), Zn(II), Ca(II) and Mg(II). Sensors and Actuators B: Chemical, 2015, 218, 25-30.	7.8	40
38	Assessment of industrial wastewater for potentially toxic elements, human health (dermal) risks, and pollution sources: A case study of Gadoon Amazai industrial estate, Swabi, Pakistan. Journal of Hazardous Materials, 2021, 419, 126450.	12.4	40
39	Solid-Contact Ion-Selective Electrodes with Highly Selective Thioamide Derivatives of <i>p</i> - <i>tert</i> -Butylcalix[4]arene for the Determination of Lead(II) in Environmental Samples. Analytical Chemistry, 2013, 85, 1555-1561.	6.5	39
40	Durable PEDOT:PSS films obtained from modified water-based inks for electrochemical sensors. Sensors and Actuators B: Chemical, 2013, 181, 694-701.	7.8	39
41	Textile-based sampling for potentiometric determination of ions. Analytica Chimica Acta, 2015, 877, 71-79.	5.4	38
42	Gold-silver nanoparticles modified electrochemical sensor array for simultaneous determination of chromium(III) and chromium(VI) in wastewater samples. Chemosphere, 2021, 281, 130880.	8.2	38
43	Progress and challenges in electrochemical sensing of volatile organic compounds using metal-organic frameworks. Critical Reviews in Environmental Science and Technology, 2019, 49, 2016-2048.	12.8	37
44	Metal-organic framework for sorptive/catalytic removal and sensing applications against nitroaromatic compounds. Journal of Industrial and Engineering Chemistry, 2020, 84, 87-95.	5.8	37
45	Solid reference electrode integrated with paper-based microfluidics for potentiometric ion sensing. Sensors and Actuators B: Chemical, 2020, 323, 128680.	7.8	37
46	Ni-Zn-based nanocomposite loaded on cordierite mullite ceramic for syngas desulfurization: Performance evaluation and regeneration studies. Chemical Engineering Journal, 2018, 351, 230-239.	12.7	36
47	Influence of surface morphology on the performance of nanostructured ZnO-loaded ceramic honeycomb for syngas desulfurization. Fuel, 2018, 211, 591-599.	6.4	35
48	<i>In Situ</i> Potentiometry and Ellipsometry: A Promising Tool to Study Biofouling of Potentiometric Sensors. Analytical Chemistry, 2016, 88, 3009-3014.	6.5	34
49	Tuned galvanostatic polarization of solid-state lead-selective electrodes for lowering of the detection limit. Analytica Chimica Acta, 2011, 707, 1-6.	5.4	33
50	Determination of Lead(II) in Groundwater Using Solid‣tate Lead(II) Selective Electrodes by Tuned Galvanostatic Polarization. Electroanalysis, 2013, 25, 123-131.	2.9	33
51	Paper-based microfluidic sampling and separation of analytes for potentiometric ion sensing. Sensors and Actuators B: Chemical, 2017, 243, 346-352.	7.8	33
52	Sal wood sawdust derived highly mesoporous carbon as prospective electrode material for vanadium redox flow batteries. Journal of Electroanalytical Chemistry, 2019, 834, 94-100.	3.8	33
53	Too small to matter? Physicochemical transformation and toxicity of engineered nTiO2, nSiO2, nZnO, carbon nanotubes, and nAg. Journal of Hazardous Materials, 2021, 404, 124107.	12.4	33
54	Catalytic processing of non-condensable pyrolysis gas from plastics: Effects of calcium supports on nickel-catalyzed decomposition of hydrocarbons and HCl sorption. Chemical Engineering Science, 2018, 189, 311-319.	3.8	32

#	Article	IF	CITATIONS
55	Paper as sampling substrates and all-integrating platforms in potentiometric ion determination. TrAC - Trends in Analytical Chemistry, 2020, 133, 116070.	11.4	32
56	Environmental footprint of voltammetric sensors based on screen-printed electrodes: An assessment towards "green―sensor manufacturing. Chemosphere, 2021, 278, 130462.	8.2	32
57	Reliable environmental trace heavy metal analysis with potentiometric ion sensors - reality or a distant dream. Environmental Pollution, 2021, 289, 117882.	7.5	32
58	Flexible conducting polymer-based cellulose substrates for on-skin applications. Materials Science and Engineering C, 2020, 108, 110392.	7.3	31
59	Recovery of nanomolar detection limit of solid-contact lead (II)-selective electrodes by electrode conditioning. Journal of Solid State Electrochemistry, 2012, 16, 2983-2991.	2.5	30
60	Catalytic activities and resistance to HCl poisoning of Ni-based catalysts during steam reforming of naphthalene. Applied Catalysis A: General, 2018, 557, 25-38.	4.3	29
61	Barium aluminate improved iron ore for the chemical looping combustion of syngas. Applied Energy, 2020, 272, 115236.	10.1	29
62	Analytical assessment of tar generated during gasification of municipal solid waste: Distribution of GC–MS detectable tar compounds, undetectable tar residues and inorganic impurities. Fuel, 2020, 268, 117348.	6.4	29
63	Cobalt ferrite nanoparticle-loaded nitrogen-doped carbon sponge as a magnetic 3D heterogeneous catalyst for monopersulfate-based oxidation of salicylic acid. Chemosphere, 2021, 267, 128906.	8.2	29
64	Near real-time analysis of para-cresol in wastewater with a laccase-carbon nanotube-based biosensor. Chemosphere, 2021, 269, 128699.	8.2	29
65	Cobalt and nitrogen co-doped porous carbon/carbon nanotube hybrids anchored with nickel nanoparticles as high-performance electrocatalysts for oxygen reduction reactions. Nanoscale, 2020, 12, 13028-13033.	5.6	29
66	Human exposure and risk assessment of recycling incineration bottom ash for land reclamation: A showcase coupling studies of leachability, transport modeling and bioaccumulation. Journal of Hazardous Materials, 2020, 385, 121600.	12.4	28
67	The properties of particleboard composites made from three sorghum (Sorghum bicolor) accessions using maleic acid adhesive. Chemosphere, 2022, 290, 133163.	8.2	28
68	Co-complexation effects during incineration bottom ash leaching via comparison of measurements and geochemical modeling. Journal of Cleaner Production, 2018, 189, 155-168.	9.3	27
69	Distribution and modeling of tar compounds produced during downdraft gasification of municipal solid waste. Renewable Energy, 2019, 136, 1294-1303.	8.9	27
70	Advances in Antiviral Material Development. ChemPlusChem, 2020, 85, 2105-2128.	2.8	27
71	Interaction between SO2 and NO in their adsorption and photocatalytic conversion on TiO2. Chemosphere, 2020, 249, 126136.	8.2	27
72	Influence of phosphate buffer and proteins on the potentiometric response of a polymeric membrane-based solid-contact Pb(II) ion-selective electrode. Electrochimica Acta, 2017, 252, 490-497.	5.2	26

#	Article	IF	CITATIONS
73	The advanced sensing systems for NO based on metal-organic frameworks: Applications and future opportunities. TrAC - Trends in Analytical Chemistry, 2020, 122, 115730.	11.4	26
74	Ba–Al-decorated iron ore as bifunctional oxygen carrier and HCl sorbent for chemical looping combustion of syngas. Combustion and Flame, 2021, 223, 230-242.	5.2	26
75	Flexible packaging plastic waste – environmental implications, management solutions, and the way forward. Current Opinion in Chemical Engineering, 2021, 32, 100684.	7.8	26
76	Multiwall carbon nanotubes derived from plastic packaging waste as a highâ€performance electrode material for supercapacitors. International Journal of Energy Research, 2021, 45, 19611-19622.	4.5	26
77	Electrochemical Behaviour of Poly(benzopyrene) Films Doped with Eriochrome Black T as a Pb ²⁺ ensitive Sensors. Electroanalysis, 2010, 22, 2794-2800.	2.9	25
78	A study on lowering the detection limit with solid-state lead-selective electrodes. Talanta, 2010, 83, 436-440.	5.5	25
79	Silver(I)-selective electrodes based on rare earth element double-decker porphyrins. Sensors and Actuators B: Chemical, 2020, 305, 127311.	7.8	25
80	Graphene-like carbon nanosheets grown over alkali-earth metal oxides: Effects of chemical composition and physico-chemical properties. Carbon, 2020, 159, 378-389.	10.3	25
81	Heteroatom doped carbon nanosheets from waste tires as electrode materials for electrocatalytic oxygen reduction reaction: Effect of synthesis techniques on properties and activity. Carbon, 2020, 167, 104-113.	10.3	25
82	Technical and environmental assessment of laboratory scale approach for sustainable management of marine plastic litter. Journal of Hazardous Materials, 2022, 421, 126717.	12.4	25
83	Coordination polymer-derived cobalt-embedded and N/S-doped carbon nanosheet with a hexagonal core-shell nanostructure as an efficient catalyst for activation of oxone in water. Journal of Colloid and Interface Science, 2020, 579, 109-118.	9.4	25
84	Electrochemically controlled transport of anions across polypyrrole-based membranes. Journal of Membrane Science, 2019, 581, 50-57.	8.2	24
85	Insights into the single and binary adsorption of copper(II) and nickel(II) on hexagonal boron nitride: Performance and mechanistic studies. Journal of Environmental Chemical Engineering, 2019, 7, 102872.	6.7	24
86	Kinetics and modeling of trace metal leaching from bottom ashes dominated by diffusion or advection. Science of the Total Environment, 2020, 719, 137203.	8.0	24
87	Ultrafine cobalt nanoparticle-embedded leaf-like hollow N-doped carbon as an enhanced catalyst for activating monopersulfate to degrade phenol. Journal of Colloid and Interface Science, 2022, 606, 929-940.	9.4	24
88	High temperature slagging gasification of municipal solid waste with biomass charcoal as a greener auxiliary fuel. Journal of Hazardous Materials, 2022, 423, 127057.	12.4	24
89	Multicalibrational procedure for more reliable analyses of ions at low analyte concentrations. Electrochimica Acta, 2014, 140, 27-32.	5.2	23
90	Progress and Challenges on Battery Waste Management :A Critical Review. ChemistrySelect, 2020, 5, 6182-6193.	1.5	23

#	Article	IF	CITATIONS
91	Weakening the strong Fe-La interaction in A-site-deficient perovskite via Ni substitution to promote the thermocatalytic synthesis of carbon nanotubes from plastics. Journal of Hazardous Materials, 2021, 403, 123642.	12.4	23
92	Chemical looping combustion-adsorption of HCl-containing syngas using alkaline-earth coated iron ore composites for simultaneous purification and combustion enhancement. Chemical Engineering Journal, 2021, 417, 129226.	12.7	23
93	Upcycling of exhausted reverse osmosis membranes into value-added pyrolysis products and carbon dots. Journal of Hazardous Materials, 2021, 419, 126472.	12.4	23
94	Metal organic frameworks (MOFs): Current trends and challenges in control and management of air quality. Korean Journal of Chemical Engineering, 2019, 36, 1839-1853.	2.7	22
95	In situ catalytic reforming of plastic pyrolysis vapors using MSW incineration ashes. Environmental Pollution, 2021, 276, 116681.	7.5	22
96	Cold-modified paper as microfluidic substrates with reduced biofouling in potentiometric ion sensing. Sensors and Actuators B: Chemical, 2021, 344, 130200.	7.8	22
97	New polyacrylate-based lead(II) ion-selective electrodes. Mikrochimica Acta, 2009, 164, 293-297.	5.0	21
98	Metal-complexed covalent organic frameworks derived N-doped carbon nanobubble–embedded cobalt nanoparticle as a magnetic and efficient catalyst for oxone activation. Journal of Colloid and Interface Science, 2021, 591, 161-172.	9.4	21
99	Conversion of Spent Coffee Beans to Electrode Material for Vanadium Redox Flow Batteries. Batteries, 2018, 4, 56.	4.5	20
100	A novel real-time monitoring and control system for waste-to-energy gasification process employing differential temperature profiling of a downdraft gasifier. Journal of Environmental Management, 2019, 234, 65-74.	7.8	20
101	Regenerable Co-ZnO-based nanocomposites for high-temperature syngas desulfurization. Fuel Processing Technology, 2020, 201, 106344.	7.2	20
102	Support effects on thermocatalytic pyrolysis-reforming of polyethylene over impregnated Ni catalysts. Applied Catalysis A: General, 2021, 622, 118222.	4.3	20
103	Upgrading waste plastic derived pyrolysis gas via chemical looping cracking–gasification using Ni–Fe–Al redox catalysts. Chemical Engineering Journal, 2022, 438, 135580.	12.7	20
104	Tuned ionophore-based bi-membranes for selective transport of target ions. Journal of Membrane Science, 2016, 511, 76-83.	8.2	19
105	Nickel-based catalysts for steam reforming of naphthalene utilizing gasification slag from municipal solid waste as a support. Fuel, 2019, 254, 115561.	6.4	19
106	Vertical distribution of heavy metals in seawater column during IBA construction in land reclamation – Re-exploration of a large-scale field trial experiment. Science of the Total Environment, 2019, 654, 356-364.	8.0	19
107	Hierarchical ZIF-decorated nanoflower-covered 3-dimensional foam for enhanced catalytic reduction of nitrogen-containing contaminants. Journal of Colloid and Interface Science, 2021, 602, 95-104.	9.4	19
108	One-pot synthesis of reduced graphene oxide/chitosan/zinc oxide ternary nanocomposites for supercapacitor electrodes with enhanced electrochemical properties. Materials Letters, 2022, 314, 131846.	2.6	19

#	Article	IF	CITATIONS
109	Nernstâ€Planckâ€Poisson Model for the Description of Behaviour of Solidâ€Contact Ionâ€Selective Electrodes at Low Analyte Concentration. Electroanalysis, 2013, 25, 133-140.	2.9	18
110	Synthesis of CaCr2O4/carbon nanoplatelets from non-condensable pyrolysis gas of plastics for oxygen reduction reaction and charge storage. Journal of Electroanalytical Chemistry, 2019, 849, 113368.	3.8	18
111	On-line microcolumn-based dynamic leaching method for investigation of lead bioaccessibility in shooting range soils. Chemosphere, 2020, 256, 127022.	8.2	18
112	Ion selective electrodes utilizing a ferrocyanide doped redox active screen-printed solid contact - impact of electrode response to conditioning. Journal of Electroanalytical Chemistry, 2020, 870, 114262.	3.8	18
113	Iron ore modified with alkaline earth metals for the chemical looping combustion of municipal solid waste derived syngas. Journal of Cleaner Production, 2021, 282, 124467.	9.3	18
114	Dualism of Sensitivity and Selectivity of Porphyrin Dimers in Electroanalysis. Analytical Chemistry, 2017, 89, 3943-3951.	6.5	17
115	Effective H2S control during chemical looping combustion by iron ore modified with alkaline earth metal oxides. Energy, 2021, 218, 119548.	8.8	17
116	Converting polyolefin plastics into few-walled carbon nanotubes via a tandem catalytic process: Importance of gas composition and system configuration. Journal of Hazardous Materials, 2022, 435, 128949.	12.4	17
117	Oxygen carriers from incineration bottom ash for chemical looping combustion of syngas: Effect of composition on combustion efficiency. Chemical Engineering Journal, 2021, 405, 127068.	12.7	16
118	Characterization of nano-layered solid-contact ion selective electrodes by simultaneous potentiometry and quartz crystal microbalance with dissipation. Analytica Chimica Acta, 2020, 1128, 19-30.	5.4	15
119	Fe-assisted catalytic chemical vapor deposition of graphene-like carbon nanosheets over SrO. Carbon, 2021, 171, 444-454.	10.3	15
120	Advanced Ni tar reforming catalysts resistant to syngas impurities: Current knowledge, research gaps and future prospects. Fuel, 2022, 318, 123602.	6.4	15
121	Dual-functional witherite in improving chemical looping performance of iron ore and simultaneous adsorption of HCl in syngas at high temperature. Chemical Engineering Journal, 2021, 413, 127538.	12.7	14
122	Nitrogen-containing carbon hollow nanocube-confined cobalt nanoparticle as a magnetic and efficient catalyst for activating monopersulfate to degrade a UV filter in water. Journal of Environmental Chemical Engineering, 2022, 10, 106989.	6.7	14
123	Tailoring Fe2O3–Al2O3 catalyst structure and activity via hydrothermal synthesis for carbon nanotubes and hydrogen production from polyolefin plastics. Chemosphere, 2022, 297, 134148.	8.2	14
124	Effects of different biochars on physicochemical properties and immobilization of potentially toxic elements in soil - A geostatistical approach. Chemosphere, 2021, 277, 130350.	8.2	13
125	Few-walled carbon nanotubes derived from shoe waste plastics: Effect of feedstock composition on synthesis, properties and application as CO2 reduction electrodes. Journal of Cleaner Production, 2022, 356, 131868.	9.3	13
126	Impacts of pyrolysis temperatures on physicochemical and structural properties of green waste derived biochars for adsorption of potentially toxic elements. Journal of Environmental Management, 2022, 317, 115385.	7.8	13

#	Article	IF	CITATIONS
127	Gravity-driven membrane filtration of primary wastewater effluent for edible plant cultivations: Membrane performance and health risk assessment. Journal of Environmental Chemical Engineering, 2022, 10, 107046.	6.7	12
128	Non-equilibrium potentiometric sensors integrated with metal modified paper-based microfluidic solution sampling substrates for determination of heavy metals in complex environmental samples. Analytica Chimica Acta, 2022, 1197, 339495.	5.4	12
129	Modulating local environment of Ni with W for synthesis of carbon nanotubes and hydrogen from plastics. Journal of Cleaner Production, 2022, 352, 131620.	9.3	11
130	Effect of alkali earth metal doping on the CuO/Al2O3 oxygen carrier agglomeration resistance during chemical looping combustion. Journal of Cleaner Production, 2022, 366, 132970.	9.3	11
131	3-D and electrically conducting functional skin mapping for biomedical applications. Chemical Communications, 2018, 54, 980-983.	4.1	10
132	Hollow porous cobalt oxide nanobox as an enhanced for activating monopersulfate to degrade 2-hydroxybenzoic acid in water. Chemosphere, 2022, 294, 133441.	8.2	10
133	Application of bipolar electrochemistry to accelerate dew point corrosion for screening of steel materials for power boilers. Fuel, 2020, 265, 116886.	6.4	9
134	Hydrogen bromide in syngas: Effects on tar reforming, water gas-shift activities and sintering of Ni-based catalysts. Applied Catalysis B: Environmental, 2021, 280, 119435.	20.2	9
135	Artificial Neural Network (ANN) Modelling for Biogas Production in Pre-Commercialized Integrated Anaerobic-Aerobic Bioreactors (IAAB). Water (Switzerland), 2022, 14, 1410.	2.7	9
136	Characterization and comparison of gasification and incineration fly ashes generated from municipal solid waste in Singapore. Waste Management, 2022, 146, 44-52.	7.4	9
137	Thermal behavior of Cu-Mg-Al-Ba/Sr bifunctional composites during chemical looping combustion and HCl adsorption of MSW syngas. Chemical Engineering Journal, 2022, 430, 132871.	12.7	8
138	Temperature-dependent synthesis of multi-walled carbon nanotubes and hydrogen from plastic waste over A-site-deficient perovskite La0.8Ni1-xCoxO3-δ. Chemosphere, 2022, 291, 132831.	8.2	8
139	Effects of modifier (Gd, Sc, La) addition on the stability of low Ni content catalyst for dry reforming of model biogas. Fuel, 2022, 312, 122823.	6.4	8
140	A novel modified terpyridine derivative as a model molecule to study kinetic-based optical spectroscopic ion determination methods. Synthetic Metals, 2016, 219, 101-108.	3.9	7
141	Highly active and poison-tolerant nickel catalysts for tar reforming synthesized through controlled hydrothermal synthesis. Applied Catalysis A: General, 2020, 607, 117779.	4.3	7
142	Acidified paper substrates for microfluidic solution sampling integrated with potentiometric sensors for determination of heavy metals. Sensors and Actuators B: Chemical, 2021, 347, 130567.	7.8	7
143	Comparison and modeling of leachate transportation dominated by the field permeability with an an anisotropic characteristic based on a large-scale field trial study. Chemosphere, 2020, 242, 125254.	8.2	6
144	Impact of molecular linker size on physicochemical properties of assembled gold nanoparticle mono-/multi-layers and their applicability for functional binding of biomolecules. Journal of Colloid and Interface Science, 2019, 543, 307-316.	9.4	5

#	Article	lF	CITATIONS
145	Physically Tailoring Ion Fluxes by Introducing Foamlike Structures into Polymeric Membranes of Solid Contact Ion-Selective Electrodes. ACS Sensors, 2021, 6, 3667-3676.	7.8	5
146	Selfâ€Referencing Background Correction Method for Voltammetric Investigation of Reversible Redox Reaction. Electroanalysis, 2013, 25, 2054-2059.	2.9	4
147	Application of terpyridyl ligands to tune the optical and electrochemical properties of a conducting polymer. RSC Advances, 2018, 8, 29505-29512.	3.6	4
148	Polyterthiophenes Crossâ€Linked with Terpyridyl Metal Complexes for Molecular Architecture of Optically and Electrochemically Tunable Materials. ChemElectroChem, 2020, 7, 4453-4459.	3.4	4
149	Electrografting of Sterically Bulky Tetramethylaniline Groups on Glassy Carbon Electrodes through Aryldiazonium Chemistry: Reasons for the Formation of Multilayers. ChemElectroChem, 2020, 7, 3368-3380.	3.4	4
150	Nanopetal-like copper hydroxide nitrate as a highly selective heterogeneous catalyst for valorization of vanillic alcohol via oxidation. Journal of Environmental Chemical Engineering, 2021, 9, 106092.	6.7	4
151	Redistribution of mineral phases of incineration bottom ash by size and magnetic separation and its effects on the leaching behaviors. Environmental Pollution, 2021, 290, 118015.	7.5	4
152	Sorbents for high-temperature removal of alkali metals and HCl from municipal solid waste derived syngas. Fuel, 2022, 321, 124058.	6.4	4
153	The Effects of Washing Techniques on Thermal Combustion Properties of Sewage Sludge Chars. International Journal of Environmental Research, 2021, 15, 285-297.	2.3	3
154	Evolution of electrochemical potentials mediated by lipophilic salts at the buried membrane interface of solid contact ion selective electrodes. Sensors and Actuators B: Chemical, 2021, 349, 130766.	7.8	3
155	Carbon nanosheet-carbon nanocage encapsulated Cu composite from chemical vapor deposition of real-world plastic waste for tailored CO2 conversion to various products. Applied Materials Today, 2021, 25, 101207.	4.3	3
156	Unravelling the significance of catalyst reduction stage for high tar reforming activity in the presence of syngas impurities. Applied Catalysis A: General, 2022, 642, 118711.	4.3	3
157	Selective Aerobic Upgrading of Lignin-Derived Compound Using a Recyclable Dual-Functional TPO-Loaded Cu-BTC Catalyst. Waste and Biomass Valorization, 2021, 12, 673-685.	3.4	2
158	Facile synthesis of electrocatalytically active bismuth oxide nanosheets for detection of palladium traces in pharmaceutical wastewater. Environmental Pollution, 2022, 307, 119524.	7.5	2
159	Selective leaching of scandium and yttrium from red mud induced by hydrothermal treatment. Journal of Chemical Technology and Biotechnology, 2021, 96, 2620-2629.	3.2	1
160	Conversion of reverse osmosis membranes into metal-free carbocatalyst for electrochemical syngas production. Journal of CO2 Utilization, 2022, 58, 101908.	6.8	1
161	Diagnostics of skin features through 3D skin mapping based on electro-controlled deposition of conducting polymers onto metal-sebum modified surfaces and their possible applications in skin treatment. Analytica Chimica Acta, 2021, 1142, 84-98.	5.4	0
162	Selective conversion of hydroxymethylfurfural to diformylfuran using copper hydroxide nitrate with various nano-structures: a comparative study. Sustainable Energy and Fuels, 2022, 6, 276-288.	4.9	0

#	Article	IF	CITATIONS
163	Ultrasound Processâ€Enhanced Removal of the Toxic Disinfection Byâ€product Bromate from Water by Aluminum: A Comparative Study. Water Environment Research, 2022, 94, e10720.	2.7	0